$p o E / P C / 9 5 2 5 1 - - T 2$

SECOND GENERATION ADVANCED REBURNING
FOR HIGH EFFICIENCY NOx CONTROL

Progress Report No. 2 for Period
January 1 - March 31, 1996

By:
Vladimir M. Zamansky
Energy and Environmental Research Corporation
18 Mason, Irvine, CA 92718

Prepared for:
William P. Barnett
Project Manager
U.S. Department of Energy
Pittsburgh Energy Technology Center
P.O. Box 10940, MS 922-316B
Pittsburgh, PA 15236-0940

RECEIVED
USDOE/PETC
96 APR 29 AM 10: 42
ACQUISITION & ASSISTANCE DIV.

April 25, 1996

MASTER

DISCLAIMER

Portions of this document may be illegible
in electronic image products. Images are
produced from the best available original
document.

TABLE OF CONTENTS

DISCLAIMER

LIST OF FIGURES

LIST OF TABLES

1.0 Introduction

Existing NO_x control technologies have limitations which may prevent them from successfully achieving commercial, cost effective application in the near future. This project develops a family of novel NO_x control technologies, Second Generation Advanced Reburning (SGAR), which have a potential to achieve 90+% NO_x control at a significantly lower cost than SCR.

Phase I consists of six tasks:

Task 1.1 Project Coordination and Reporting/Deliverables

Task 1.2 Kinetics of Na_2CO_3 Reactions with Flue Gas Components

Task 1.3 0.1×10^6 Btu/hr Optimization Studies

Task 1.4 1.0×10^6 Btu/hr Process Development Tests

Task 1.5 Mechanism Development and Modeling

Task 1.6 Design Methodology and Application

During the first reporting period (October 1 - December 31, 1995), the Phase I Project Management Plan was prepared and the Kick-off meeting was performed at PETC. The bench-scale facility, 0.1 MBtu/hr Controlled Temperature Tower (CTT), was prepared for the experimental program (Task 1.3). Modeling (Task 1.5) was focused on selection of a C-H-O-N chemical mechanism for description of the process chemistry.

This second reporting period (January 1 - March 31, 1996) included both modeling and experimental activities. Modeling was focused on evaluation of ammonia injection into the reburning zone and on the effect of various additives on promotion of the $NO-NH_3$ interaction in the reburning zone. First bench scale CTT experiments have been performed on different variants of the AR technology. The tests are continued, and the results will be reduced and reported in the next quarter. According to the project plan, a study on high-temperature reactions of sodium promoters (Task 1.2) has to be performed at the University of Texas in Austin (UT). Subcontract negotiations between EER and UT have been completed, and the UT team started their research.

2.0 Kinetic Modeling

As was described in the 1st quarterly report (Zamansky and Maly, 1996), a detailed C-H-O-N kinetic mechanism was selected for modeling. The mechanism is based on the recently issued Version 2.11 of GRI-Mech (Bowman, Hanson et al., 1995) and includes SNCR reactions suggested by Bowman, 1995. The mechanism was presented in Appendix I of the 1st quarterly report verified by comparison with available experimental data on the Thermal DeNOx process.

During the current reporting period, modeling activities were continued with the use of the selected C-H-O-N mechanism. The following issues were addressed:

- modeling of reburning with various stoichiometric ratios in the reburning zone;

- variation of reburning fuel (RF) injection temperature;

- delayed ammonia injection into the reburning zone;

- promotion of the NO-NH_3 interaction in the reburning zone.

The CHEMKIN-II kinetic program developed at the Sandia National Laboratories (Kee et al., 1989) was used for modeling. Calculations were performed without any adjustments in rate constants taking into account an actual BSF (Boiler Simulator Facility) temperature profile which is expected to be about 300 K/s in the reburning zone.

Figure 2.1 reminds the nomenclature to refer to the various regions of the Second Generation Advanced Reburning (SGAR) process. The region upstream of the reburning fuel injection is referred to as the "primary zone". The primary zone Stoichiometric Ratio (SR_1) is maintained at $SR_1=1.1$ for all tests and the initial NO concentration in this zone is referred to by a single subscript "i". The region between the reburning fuel and overfire air (OFA) injection is referred to as the "reburning zone". The reburning fuel is injected at a temperature of T_1. The first N-agent (A_1) is introduced at T_2 with a Nitrogen Stoichiometric molar Ratio $NSR_1=A_1/NO_i$ into the reburn zone, this zone is divided into two fuel rich zones with stoichiometries SR_2 and SR_3. NO concentration upstream of the first N-agent injection is referred to as "ii". NO reduction from NO_i to NO_{ii} is caused by
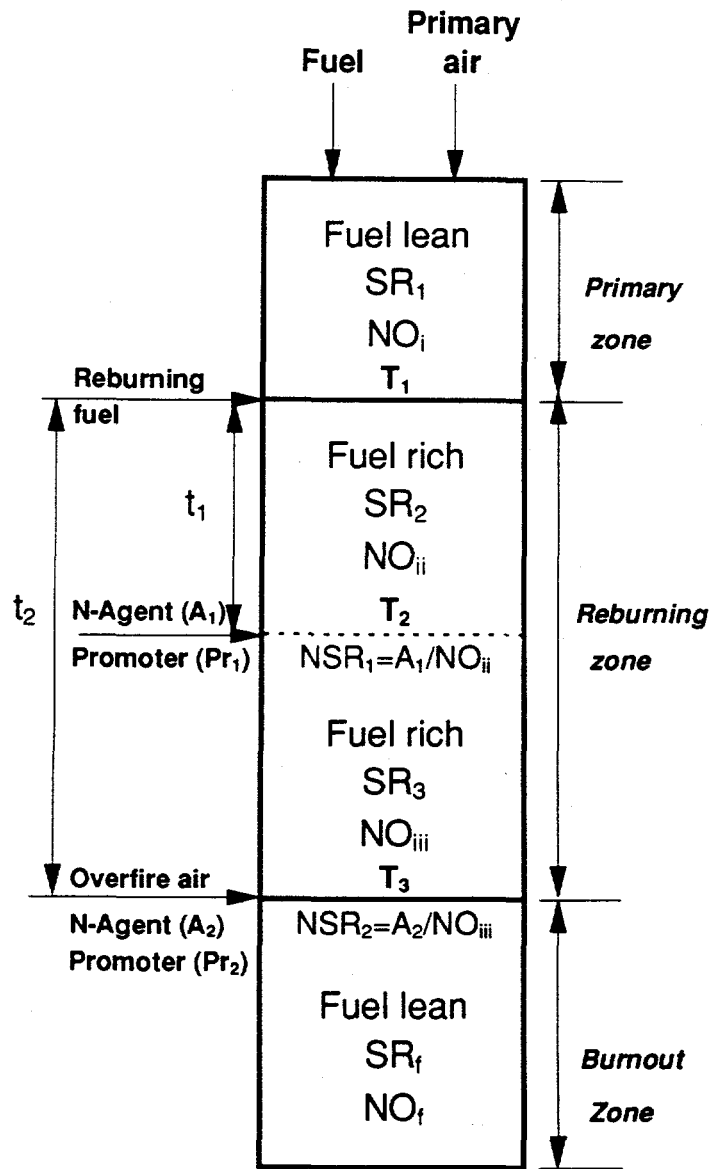
Figure 2.1   SGAR schematic - definitions.

reburning only. The first N-agent is injected with or without promoters (Pr_1) with a t_1 delay time after RF injection. NO concentration downstream of the A_1 injection is called NO_{iii}, and NO reduction from NO_i to NO_{iii} is caused by the first N-agent. Overfire air is injected at T_3 with a t_2 delay time after RF injection. OFA is a career gas for injecting the second N-agent (A_2) which is injected with or without promoters (Pr_2). A_2 is injected with $NSR_2 = A_2/NO_{iii}$. The downstream region is referred to as the "burnout zone". Stoichiometric ratio in this zone is SR_f, and the final NO concentration is NO_f.

Modeling of the SGAR process is a multi-parametric task. SGAR includes injections of 6 different components, and each injection depends on several parameters. These injections and associated parameters, varied in modeling, are the following:

1. Injection of the reburning fuel (CH_4 is considered in modeling)

    - heat input (SR_2);

    - injection temperature (T_1).

2. N-agent injection into the reburning zone (NH_3 is considered in modeling)

    - injection temperature (T_2) or delay time (t_1);

    - N-agent amount (A_1, NSR_1).

3. Promoter injection into the reburning zone

    - promoter amount (Pr_1);

    - mechanism of promotion.

4. N-agent injection into the burnout zone (NH_3 is considered in modeling)

    - injection temperature (T_3) or delay time (t_2);

    - N-agent amount (A_2, NSR_2).

5. Promoter injection into the burnout zone

    - promoter amount (Pr_2);

    - mechanism of promotion.

6. OFA injection

    - injection temperature (T_3).

A modeling approach was selected which makes it possible to model each injection separately and then optimize them simultaneously.

2.1 Injection of the Reburning Fuel

Stoichiometric ratio SR_1 in the primary zone was kept at $SR_1=1.1$ for all calculations. This SR_1 corresponds to methane combustion with the following mixture composition:

8.72% CH_4 - 19.18% O_2 - balance N_2
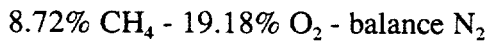
If the combustion process in the primary zone is complete, it generates about 8% CO_2 and 15% H_2O. At the same time, 1.74% O_2 is left which is available for oxidation of the reburning fuel. Table 2.1.1 presents molar fractions of methane which are necessary to provide certain stoichiometric ratios in the reburning zone.

Table 2.1.1. Concentrations of methane injected into the reburning zone.

SR_2	1	0.99	0.95	0.90	0.80	0.70
$[CH_4]$, %	0.87	0.967	1.37	1.94	3.27	4.98

Thus, to provide a desirable SR_2 in the reburning zone, one should select a certain $[CH_4]$ from Table 2.1.1 and use the following mixture:

$[CH_4]$ - 1.74% O_2 - 600 ppm NO - 8% CO_2 - 15% H_2O - balance N_2.
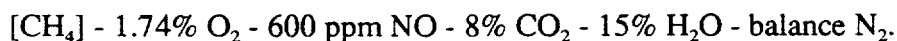
An initial NO concentration NO_i = 600 ppm was used for calculations. Figures 2.1.1-2.1.3 demonstrate concentration profiles of main species in the reburning zone at an injection temperature $T_1 = 1700$ K and SR_2 equals 0.99, 0.95, and 0.90, respectively. Comparison of these graphs shows that CH_4 is rapidly converted to CO and H_2. Only at $SR_2=0.90$, about 300 ppm CH_4 is present in the mixture. At $SR_2=0.99$ and 0.95, the amount of CH_4 is lower than 1 ppm.

5
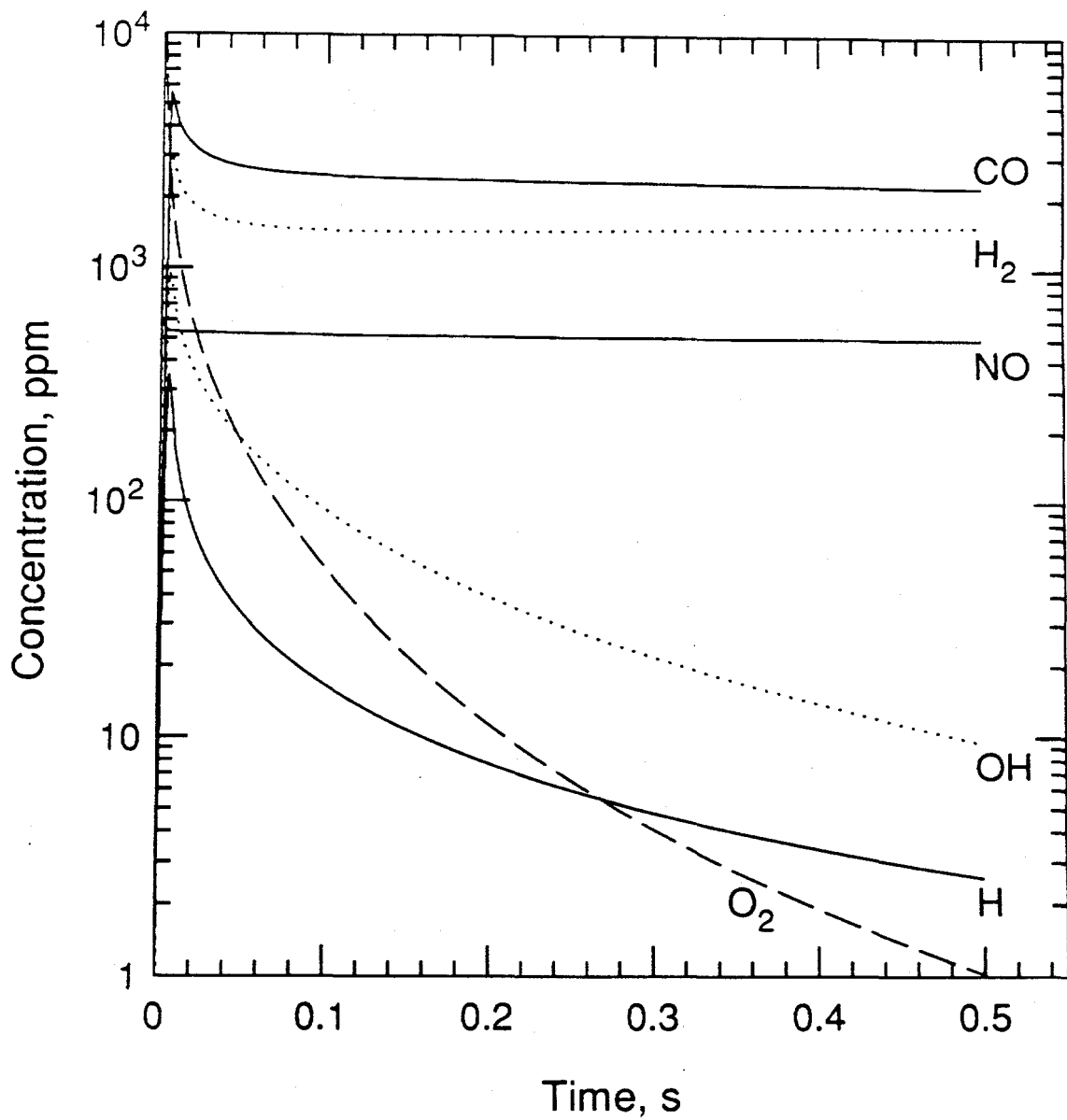
Figure 2.1.1. Kinetic curves of the main species in the reburning zone at $SR_2 = 0.99$ and injection temperature $T_1 = 1700$ K.
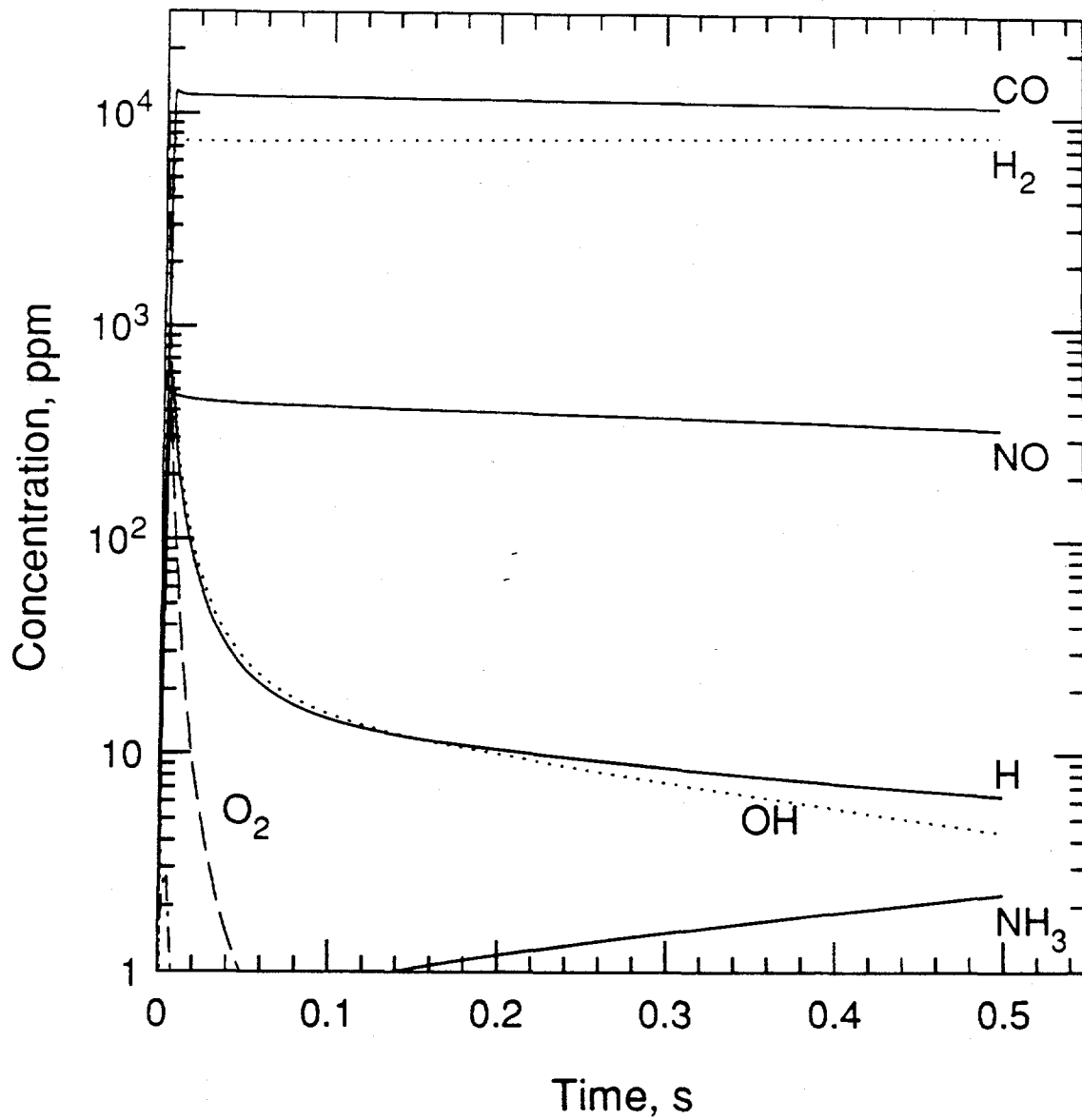
Figure 2.1.2. Kinetic curves of the main species in the reburning zone at $SR_2 = 0.95$ and injection temperature $T_1 = 1700$ K.
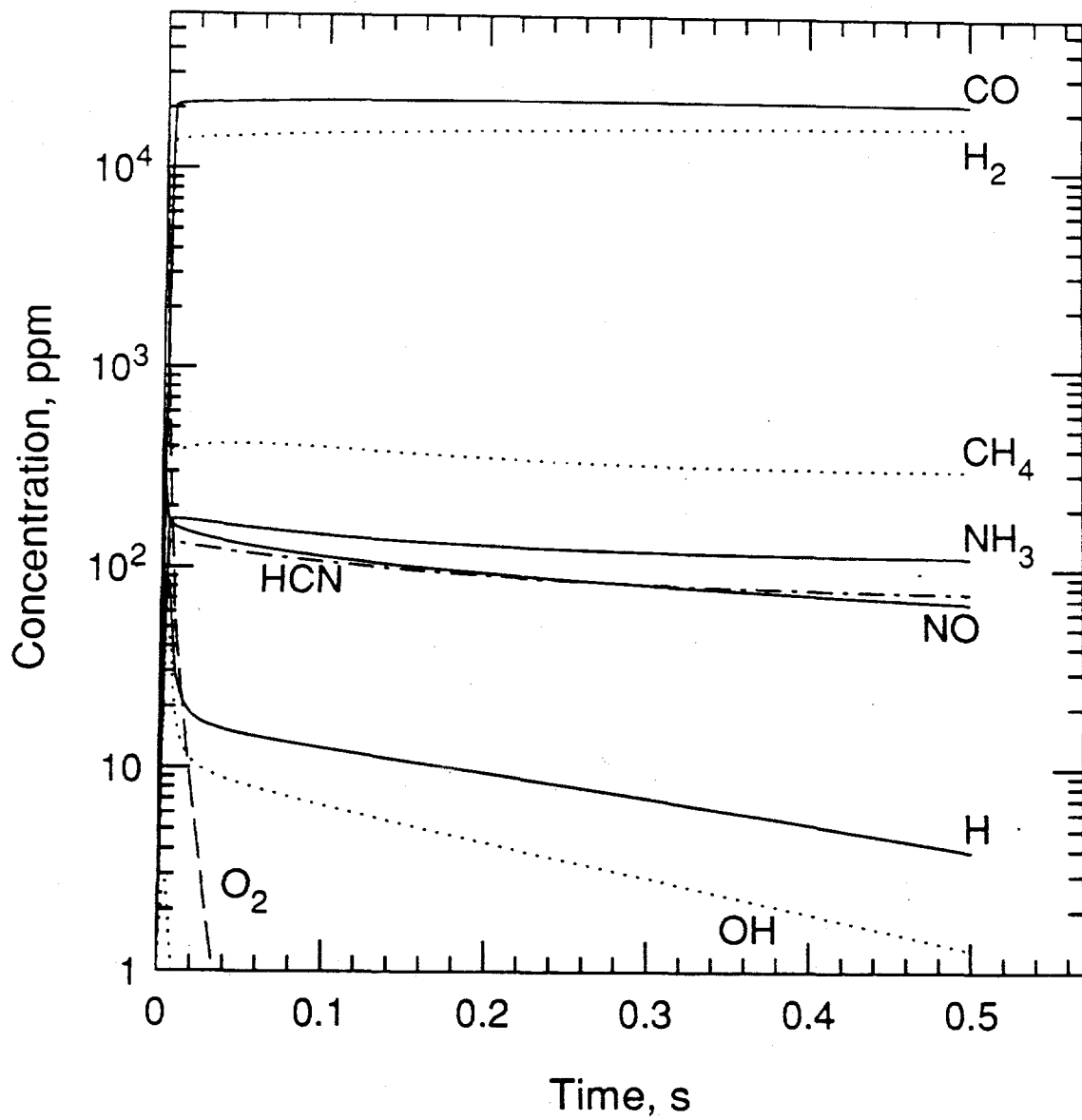
Figure 2.1.3. Kinetic curves of the main species in the reburning zone at $SR_2 = 0.90$ and injection temperature $T_1 = 1700$ K.

At $SR_2 = 0.99$ (Figure 2.1.1), NO concentration drops during very short period of time from 600 ppm to about 540 ppm and then, slowly decreases to 502 ppm. Concentrations of NH_3 and HCN are lower than 1 ppm, though some O_2 is still present.

At $SR_2 = 0.95$ (Figure 2.1.2), oxygen disappears within 0.05 s, and NH_3 concentration slowly increases. NO again rapidly drops to about 430 ppm and decay slowly to 330 ppm. Total Fuel Nitrogen (TFN = $NO+NH_3+HCN$) concentration is 332 ppm by 0.5 s.

At $SR_2 = 0.90$ (Figure 2.1.3), NO rapidly and more efficiently decreases from 600 to 160 ppm, and then slowly to 67 ppm. However, in this case, the mixture contains 75 ppm HCN and 115 ppm NH_3 at t = 0.5 s. Hence, TFN equals 257 ppm.

The results show that there are two steps of NO reduction in the reburning process: the first very fast step and the second slow step. The reason of these fast and slow decreases in NO concentration is of primary interest for understanding the reburning phenomenon. To clarify the main processes in the fast NO reduction zone, calculations were carried out with a reaction time of 5 msec for $SR_2 =$ 0.99 and 0.90. Figures 2.1.4 and 2.1.5 represent the results.

Figure 2.1.4 demonstrates kinetic curves in the reburning zone at $SR_2 = 0.99$, $T_1 = 1700$ K, and t = 5 ms. The NO concentration has even a little minimum at about 2 ms. This minimum is explained by reactions of NO with C-containing radicals: CH_3, CH_2, HCCO, $CH_2(S)$, CH, and C. The radicals are formed from CH_3 which, in turn, is formed from CH_4. The radicals participate also in recombination reactions with each other and in reactions with oxygen and other species. As a result of these processes, concentrations of the radicals increase within 2 ms, and then, since all CH_4 is consumed and there is no more feed, the concentration of C-radicals reduces, due to recombination and oxidation, by several orders of magnitude. Concentrations of HCN and NH_3 rise simultaneously with C-radicals because HCN and NH_3 are the main molecules formed due to reactions of the radicals with NO. At about 2 ms, both HCN and NH_3 are oxidized by existing oxygen into NO. Therefore, the NO concentration slightly increases. It is of interest to note that concentrations of CH_2 and HCCO reach 8-9 ppm, though CH concentration does not exceed 0.1 ppm. Main reactions of NO
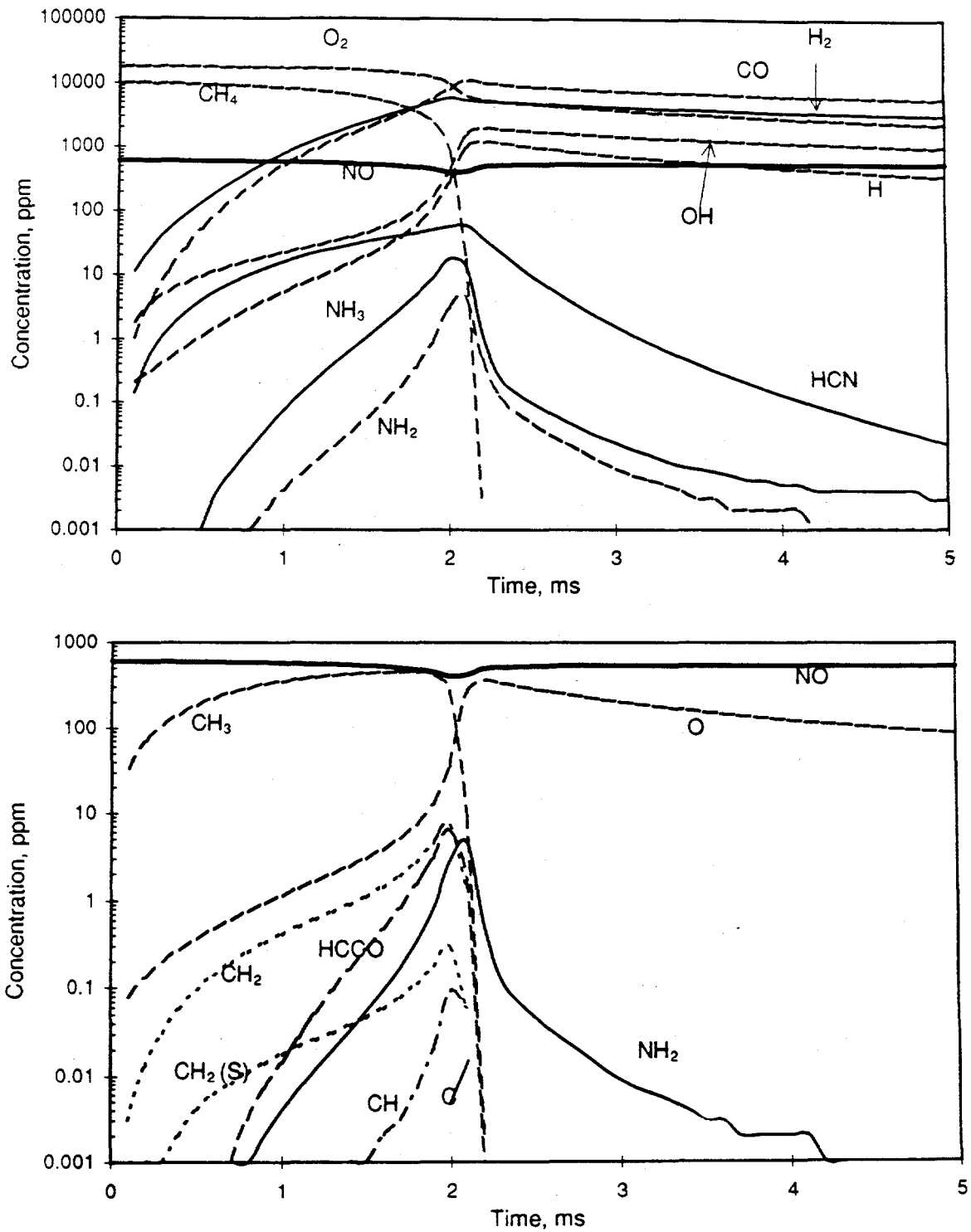
Figure 2.1.4. Kinetic curves in the reburning zone at $SR_2 = 0.99$, $T_1 = 1700$ K, and $t = 5$ ms.
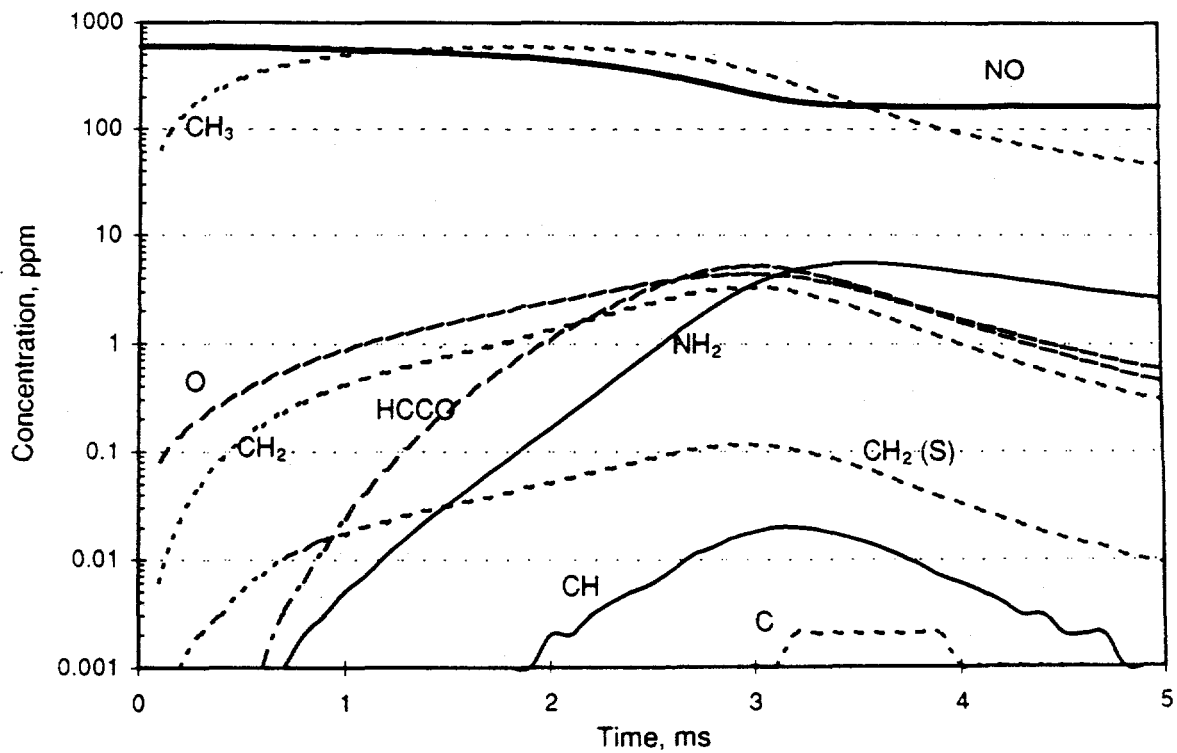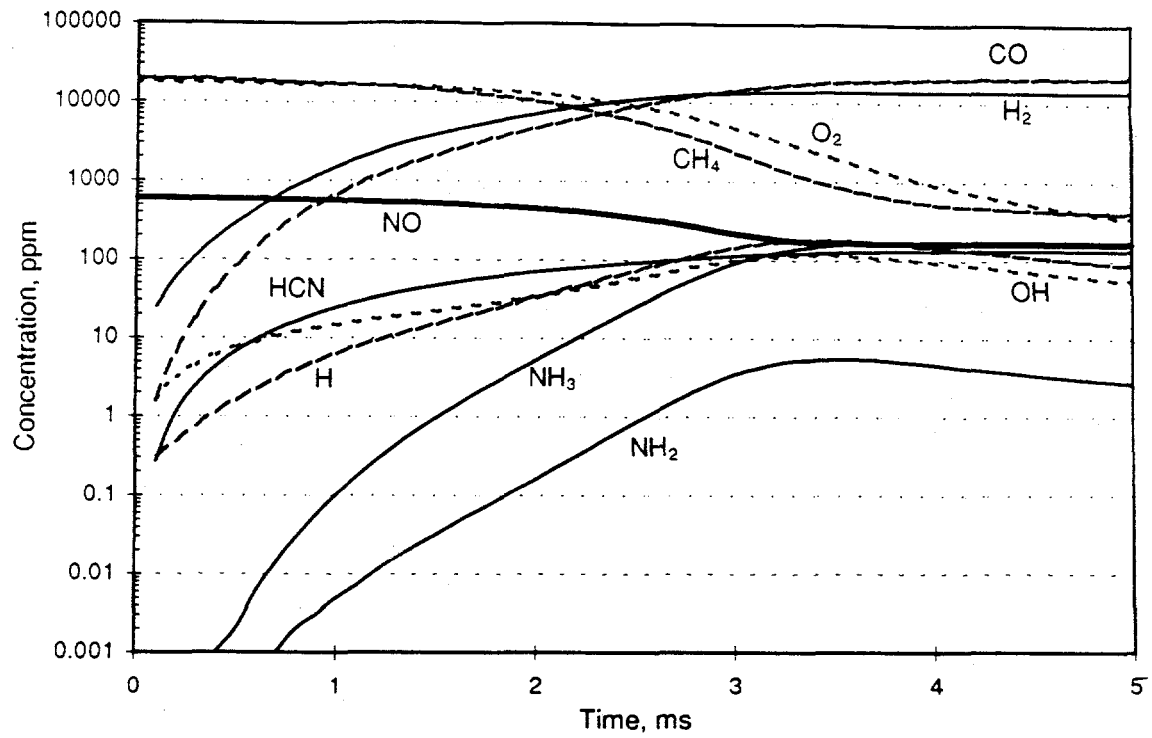
Figure 2.1.5. Kinetic curves in the reburning zone at $SR_2 = 0.90$, $T_1 = 1700$ K, and $t = 5$ ms.

11

removal can be compared by considering their rates at the maximum point of radical concentrations. Table 2.1.2 presents the NO reactions with C-radicals and their rates in arbitrary units at 2 ms.

Table 2.1.2. Comparison of NO reaction rates with C-radicals at $SR_2 = 0.99$, $T_1 = 1700K$ and t = 2 ms.

C-radical	Reaction	Rate, arb. units	Total rate, a. u.	Rank
C	C + NO = CN + O	1	2.6	6
	= CO + N	1.6		
CH	CH + NO = HCN + O	25	51	4
	= H + NCO	10		
	= N + HCO	16		
CH_2	CH_2 + NO = H + HNCO	560	900	2
	= OH + HCN	140		
	= H + HCNO	200		
$CH_2(S)$	$CH_2(S)$ + NO = H + HNCO	14	22.6	5
	= OH + HCN	3.6		
	= H + HCNO	5		
CH_3	CH_3 + NO = HCN + H_2O	71	76.6	3
	= H_2CN + OH	5.6		
HCCO	HCCO + NO = HCNO + CO	1860	1860	1

This comparison shows that HCCO radicals, followed by CH_2 radicals, are the most important species depleting NO concentration. Thus, the reactions of HCCO and CH_2 radicals are dominant pathways (in the scope of the assumed mechanism) for NO consumption during the initial fast NO removal after RF injection under the conditions examined.

Figure 2.1.5 shows kinetic curves in the reburning zone within first 5 ms at $SR_2 = 0.90$ and $T_1 = 1700$ K. NO concentration decreases from 600 to 165 ppm, and this is explained by reactions of NO with the same C-containing radicals. Concentrations of the radicals also have a maximum, in this case at about 3 ms, but they are removed not so rapidly since CH_4 concentration is much higher, and the

source of the radicals (CH_4 and CH_3) still exists within 5 ms. Concentrations of HCN and NH_3 again rise simultaneously with C-radicals, but, in this case, HCN and NH_3 are almost not oxidized since O_2 concentration drops rapidly (only 1 ppm O_2 exists in the mixture in 30 ms).

Table 2.1.3 contains reaction rates for the NO reactions with C-radicals at $SR_2 = 0.90$ at the maximum point of radical concentrations (3 ms). The same conclusion can be made: importance of NO removing radicals decreases in the row: HCCO, CH_2, CH_3, CH, $CH_2(S)$, and C.

Table 2.1.3. Comparison of NO reaction rates with C-radicals at $SR_2 = 0.90$, $T_1=1700K$ and t = 3 ms.

C-radical	Reaction	Rate, arb. units	Total rate, a. u.	Rank
C	C + NO = CN + O	1	2.6	6
	= CO + N	1.6		
CH	CH + NO = HCN + O	25		
	= H + NCO	10	51	4
	= N + HCO	16		
CH_2	CH_2 + NO = H + HNCO	553		
	= OH + HCN	139	888	2
	= H + HCNO	196		
$CH_2(S)$	$CH_2(S)$ + NO = H + HNCO	16		
	= OH + HCN	4.0	25.6	5
	= H + HCNO	5.6		
CH_3	CH_3 + NO = HCN + H_2O	200	216	3
	= H_2CN + OH	16		
HCCO	HCCO + NO = HCNO + CO	2940	2940	1

Figure 2.1.6 compares modeling and experimental data on concentrations of NO, NH_3, HCN, and TFN in the reburning zone (t = 0.5 s) at T_1 = 1700 K for different RF concentrations (various SR_2). The main difference between the experimental and modeling data sets is observed at low SR_2 where modeling predicts higher NH_3 concentration, but experiment demonstrates higher HCN level.
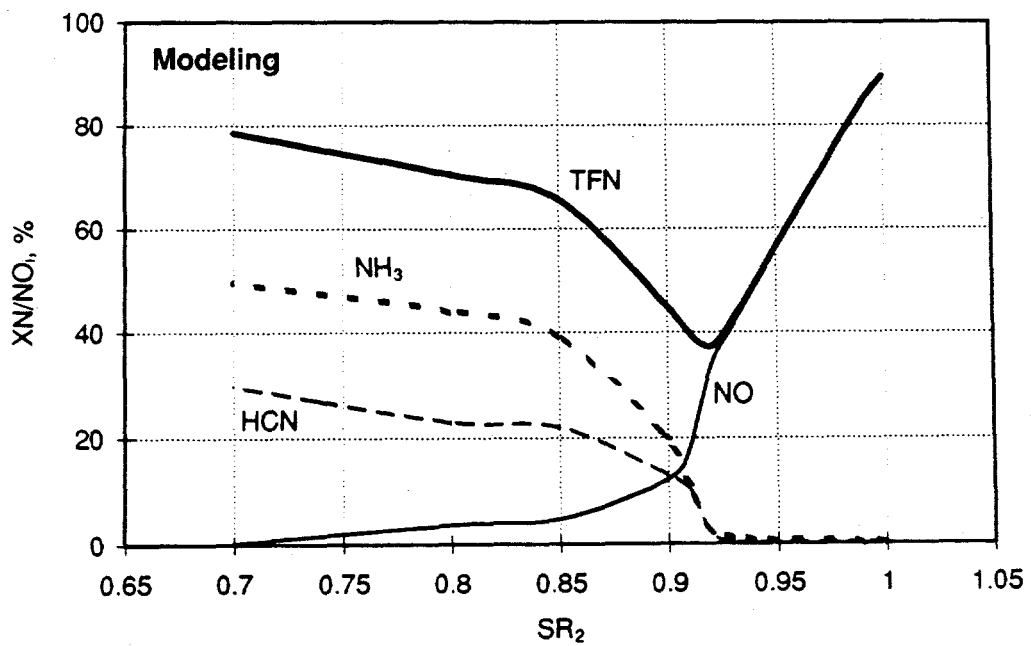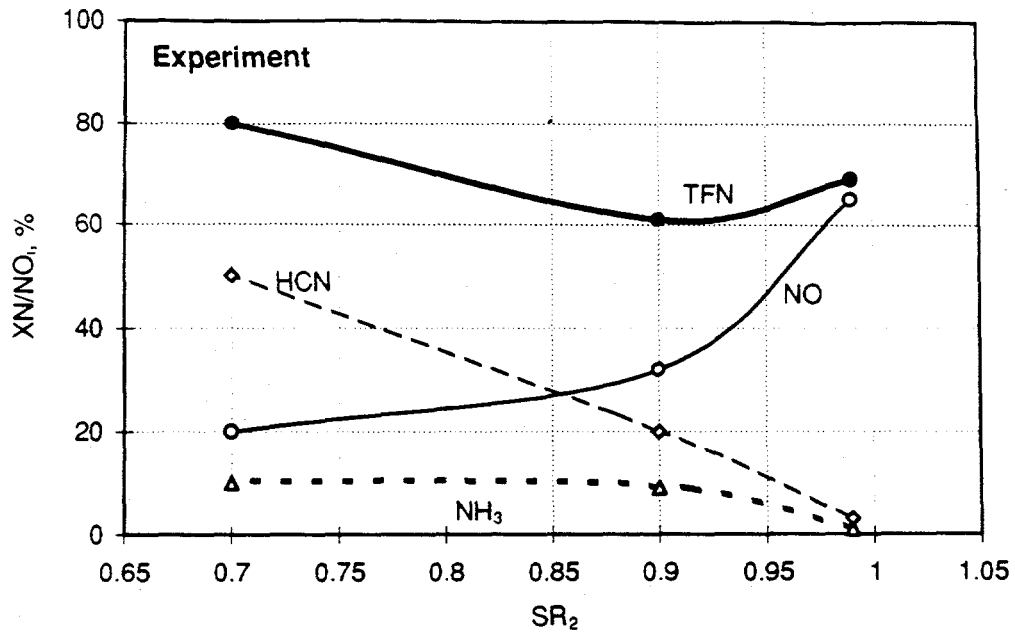
13

Figure 2.1.6. Modeling and experimental data on concentrations of NO, NH_3, HCN, and TFN in the reburning zone (t = 0.5 s) at T_1 = 1700 K for different concentrations of reburning fuel, SR_2.

14

However, at $SR_2 = 0.90$-0.99, experimental and modeling concentrations are close to each other. It worth noting that experimental data can, of course, be affected by the rate of mixing which is instant in modeling.

Figure 2.1.6 demonstrates the current level of confidence in kinetic mechanisms developed for modeling of reburning. A lot of work needs to be done to improve the model, but the model can predict major reaction trends and can help to find prospective conditions of NO removal. These conditions should be, of course, optimized by experiments.

Figure 2.1.7 compares performance of the reburning process at different temperatures for $SR_2 = 0.99$, 0.95, and 0.90. Under conditions close to stoichiometry, $SR_2 = 0.99$, concentrations of NH_3 and HCN in the reburning zone are less than 1 ppm, and all TFN is in the form of NO. TFN concentration in the reburning zone is decreased by 20-30%, and it is smaller at lower temperatures where C-radicals exist longer. Since they do not disappear too fast, more C-radicals are available for the reactions with NO. For instance, as shown in Figure 2.1.4, the first, fast reburning stage proceeds within 5 ms at $T = 1700$ K, mainly within 2 ms. At 1500 K, C-radicals do not disappear so fast, and the first stage proceeds longer, within about 20 ms. As a result, NO concentration drops in this fast stage from 600 to 535 ppm at 1700 K, but at 1500 K the process is more efficient: NO decreases from 600 to 450 ppm.

At $SR_2 = 0.95$ (Figure 2.1.7), only small amounts of NH_3 and HCN are formed at about 1500 K, and most of TFN exists in the form of NO. TFN concentration again lower at low temperatures, and it is within 40-65% TFN reduction range. At $T_1 = 1500$ K, the fast reburning stage proceeds in about 30-40 ms, much slower than at 1700 K (5 ms). The slower reactions of C-radicals cause more efficient first reburning stage: NO concentration decreases from 600 to 475 ppm and from 600 to 300 ppm at 1700 and 1500 K, respectively.

At higher RF injection rate (Figure 2.1.7, $SR_2 = 0.90$) most of NO is converted to NH_3 and HCN. Efficiency of TFN removal is 20-55%, and, in the contrary to the previous cases, TFN removal is more efficient at higher temperatures. Explanation of this effect is straightforward. At $SR_2 = 0.90$,
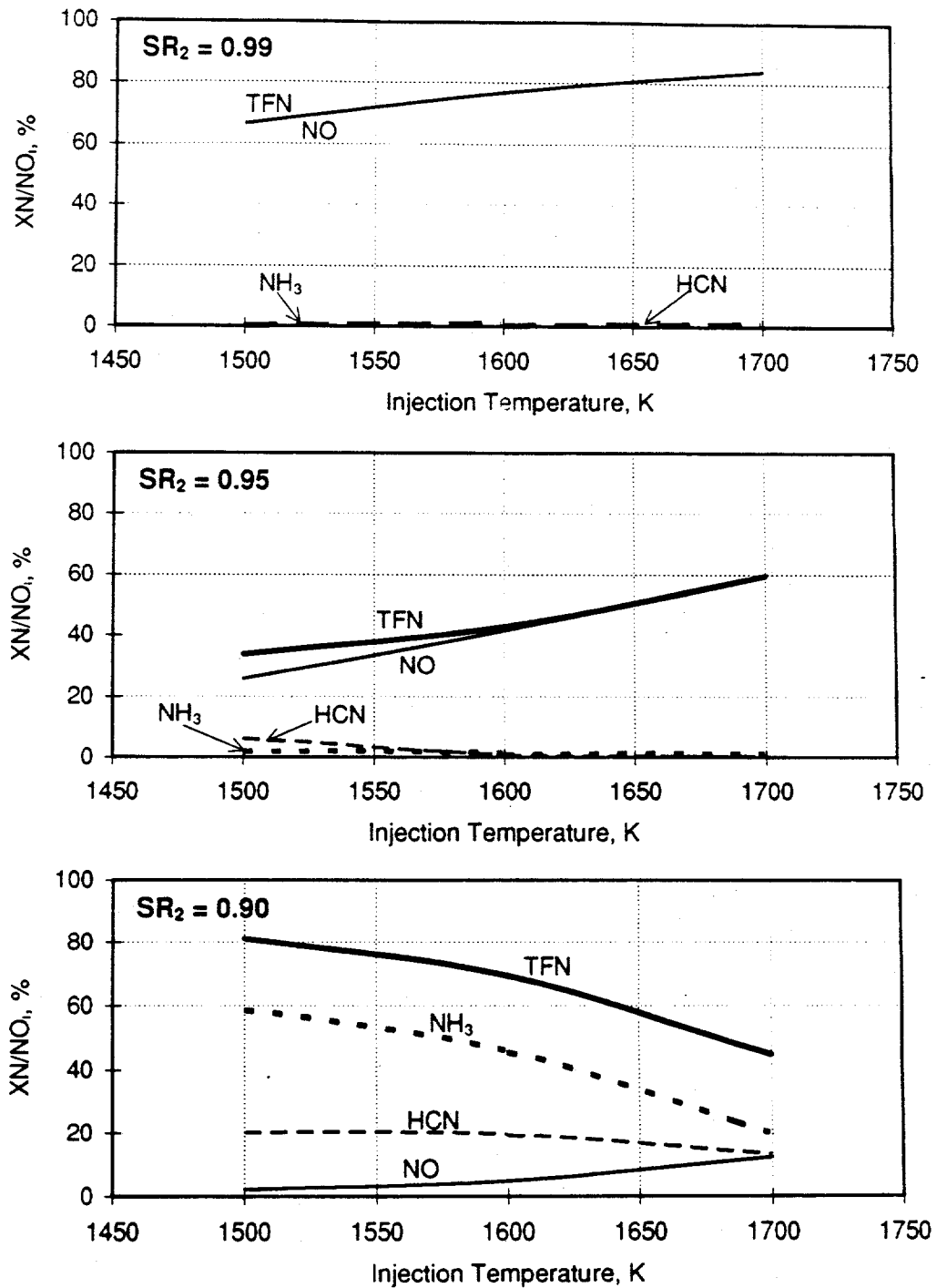
Figure 2.1.7. Modeling data on concentrations of NO, NH_3, HCN, and TFN in the reburning zone (t = 0.5 s) at T_1 = 1500-1700 K for different concentrations of reburning fuel, SR_2.

16

the efficiency of NO removal continues to increase, as seen in Figure 2.1.7, and NO level is smaller at low temperatures. However, concentrations of NH_3 and HCN are much higher than NO, and they decrease at higher temperatures since they react faster. Therefore, TFN decreases at T = 1700 K.

Thus, modeling shows that at higher RF injection rates (SR_2 is about 0.90), higher temperatures results in higher efficiency of TFN removal. At lower injection rates (SR_2 = 0.95-0.99), reburning efficiency is higher at lower temperatures. This effect can be checked and optimized by experimental testing.

2.2 Injection of Ammonia into the Reburning Zone

When fuel is added into the reburning zone, the oxygen disappears very fast in the reaction with the fuel to form CO and H_2. If N-agents (ammonia, urea, etc.) are injected into the reburning zone, they form NH_i radicals (NH_2, NH, N) which are active in NO removal reactions. The NH_i radicals can react either with O_2 into NO or with NO into N_2. The NO reduction process is effective if the NH_i precursors (N-agents) appear in the gas mixture when concentration of oxygen has been significantly depleted by the reburning fuel, thus preventing oxidation of N-agents into NO. Calculated characteristic times for O_2 disappearance after RF injection are less than 0.01 s at 1700 K and about 0.1 s at 1450 K. The delay time between RF injection and the formation of NH_i species should be close to these times for effective NO reduction.

Results of calculations which demonstrate the effect of the delayed ammonia injection on NO reduction by CH_4 reburning are presented in Figure 2.2.1. The first graph shows concentrations of NO, NH_3, HCN, and TFN after 0.5 s at different values of SR_2 for injection of 600 ppm NH_3 without delay, i.e. co-injection with the reburning fuel. At SR_2 = 0.90, ammonia co-injection causes a decrease in TFN from 1200 ppm (600 ppm NO and 600 ppm NH_3) to 327 ppm. At SR_2 = 0.90, the concentration of the reburning fuel is high, and its reaction with the oxygen forms a large radical pool. The radicals initiate a rapid reaction between NH_3 and NO, and the TFN concentration is depleted. This reaction requires a small amount of oxygen, to support the radical pool, and this amount is available in the mixture during the first rapid reaction stage. Concentration of ammonia decreases
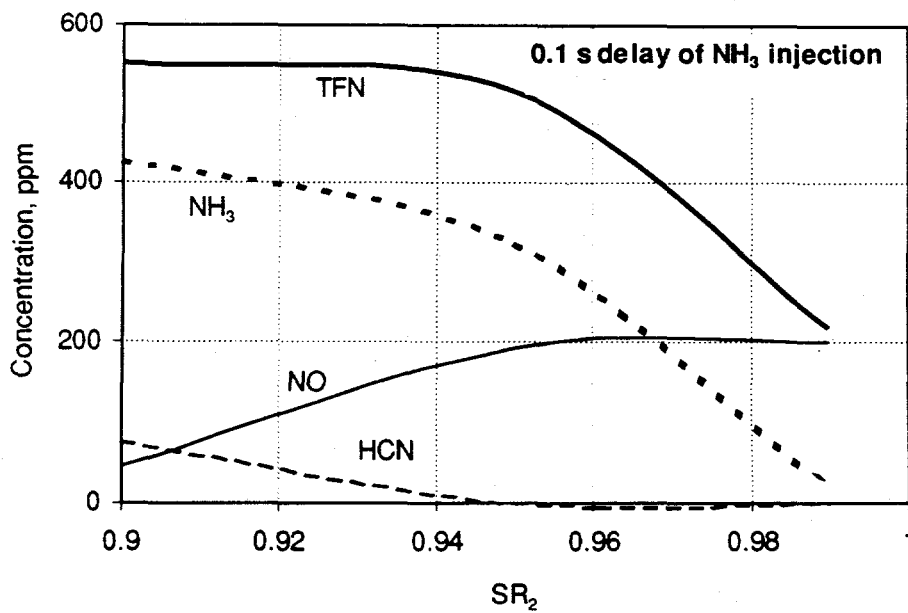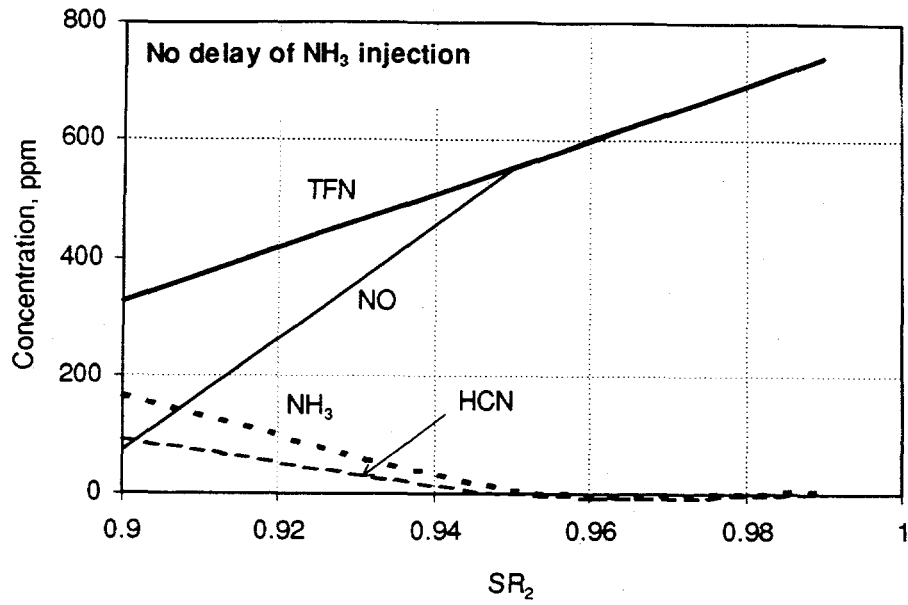
17

Figure 2.2.1. Effect of ammonia co-injection with the reburning fuel and 0.1 s delayed NH_3 injection on fuel-N species in the reburning zone. $[NH_3] = 600$ ppm, $NO_i = 600$ ppm, $T_1 = 1700$ K.

slowly at $SR_2 = 0.90$ since most of the oxygen reacts with the high concentration of CH_4. Some CH_4 (about 400 ppm) remains unreacted in the reburning zone. At $SR_2 = 0.99$, all NH_3 and CH_4 are instantly oxidized since the concentration of O_2 is the same, but the [CH_4] level is much lower. In this oxidation process, ammonia forms some additional NO, and this NO cannot be decreased in the reaction with ammonia since it is no longer present in the mixture. Therefore, TFN = NO_i = 742 ppm, i.e. the NO concentration increases.

The picture is completely different if ammonia is injected with a 0.1 s delay time, second graph in Figure 2.2.1. In this case, at $SR_2 = 0.90$, ammonia is injected when the O_2 concentration is already reduced to zero (about 0.01 ppm). Concentration of NO is reduced in the first rapid reburning stage within the delay time of 0.1 s and it decreases further utilizing some ammonia. However, in 0.5 s the NH_3 concentration is still high, about 420 ppm, and it does not react rapidly with NO since there is no oxygen to feed the radical pool. At $SR_2 = 0.99$, NH_3 is injected when the O_2 concentration is about 50 ppm (see [O_2] in Figure 2.1.1 at t = 0.1 s) and the OH concentration is still high. Therefore, in the presence of this oxygen level, NH_3 and NO are capable of reacting with each other, and TFN concentration efficiently decreases. Thus, delayed ammonia injection can result, under certain conditions, in more effective NO removal. These conditions require the presence of the both reagents and some oxygen.

The effect of the delayed ammonia injection depends on many factors, such as the value of SR_2, the delay time, ammonia concentration, oxygen concentration, etc. Figure 2.2.2 presents concentrations of fuel-N species in the reburning zone at $SR_2 = 0.99$ and various delay times of ammonia injection. This graph and concentration profiles of the main species help to explain the effect of ammonia on NO removal. If ammonia is injected along with the reburning fuel, it rapidly disappears in the reaction with the high amount of oxygen and causes some NO formation. As was demonstrated in Section 2.1, the initial stage of reburning is fast and forms high concentrations of radicals. Therefore, injection of ammonia with a short delay time results in NH_3-O_2 interaction in the presence of the radicals and small amounts of oxygen. This interaction efficiently reduces concentrations of NO and TFN. If ammonia is injected with a longer delay time, NH_3 and NO interact in the media with lower radical (and O_2) concentrations. As a result, the efficiency of NO and TFN removal is lower.
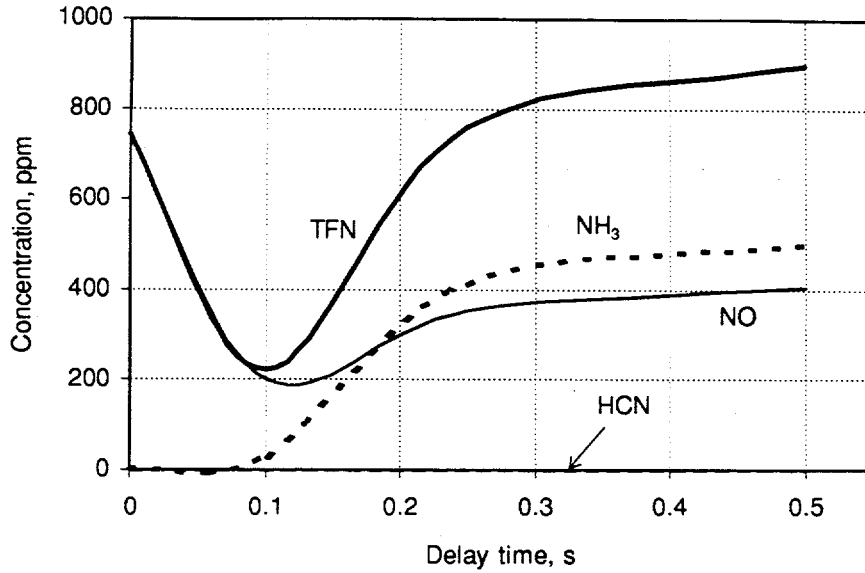
19

Figure 2.2.2. Effect of the delay time of NH_3 injection into the reburning zone at $SR_2 = 0.99$. Other conditions are the same as in Figure 2.2.1.
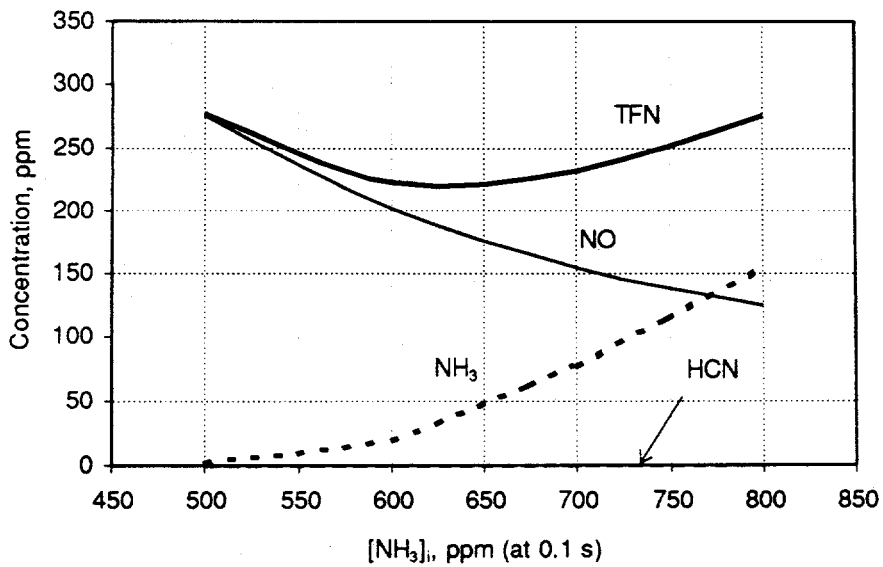

Figure 2.2.3. Effect of the NH_3 concentration injected into the reburning zone at $SR_2 = 0.99$ and 0.1 s delay time. Other conditions are the same as in Figure 2.2.1.

20

Figure 2.2.3 demonstrates how NO and TFN depend on NH_3 concentration injected with a 0.1 s delay time at $SR_2 = 0.99$. At a higher level of $[NH_3]$ injected, the NO concentration decreases, but the residual $[NH_3]$ increases. The TFN concentration has a minimum which approximately corresponds to equimolecular amounts of NO and NH_3 in the gas mixture ($NSR_1 = 1.0 - 1.3$).

Figure 2.2.4 compares performance of the reburning process at $SR_2 = 0.99$ in the presence of NH_3 in the reburning zone under different conditions of NH_3 injection (curves 1-4). Curve 1 is the initial uncontrolled NO level of 600 ppm. Curve 2 models basic reburning at $SR_2 = 0.99$ when CH_4 is added to the reburning zone at 1700 K. The NO concentration decreases to 412 ppm in 1.5 s (the time of OFA addition at 1255 K), or about 31% NO reduction. Curve 3 shows that if 800 ppm NH_3 is added simultaneously with the reburning fuel, the NO concentration is rapidly increased to 900 ppm and then reduced to 500 ppm in 1.5 s. Thus, the addition of NH_3 in the presence of oxygen initially increases the NO concentration, but by the time of OFA injection, [NO] is close to the level achieved by the basic reburning process. High oxygen concentration prevents NO reduction because the added NH_3 burns rapidly in the presence of O_2 to form additional NO. If ammonia is added not with the reburning fuel, but after the O_2 concentration has decreased through reaction with the reburning fuel, the efficiency of NO removal is much higher: 0.1 s delayed NH_3 injection in curve 4. In 1.5 s of the reaction time, the NO concentration drops to 113 ppm, but 144 ppm NH_3 is left in the reaction media, and thus, TFN = 257 ppm as shown in Figure 2.2.4. Concentration of HCN was below 1 ppm under all process conditions with $SR_2 = 0.99$. Injection of OFA at 1255 K resulted in 230 ppm final NO concentration, 62% NO reduction.

At higher RF concentration ($SR_2 = 0.90$), modeling shows formation of 229 ppm TFN in 1.5 s (70 ppm HCN, 115 ppm NH_3, and 44 ppm NO). Injection of OFA at 1255 K results in a 200 ppm final NO level, corresponding to 67% NO reduction. Injection of ammonia ($NSR_1 = 1.5$) into the fuel-rich zone at $SR_2 = 0.9$ with a 0.1 s delay time followed by OFA injection, does not significantly change the final NO level. Thus, injection of N-agents into the reburning zone is more efficient under near stoichiometric conditions. At higher reburning fuel levels, concentrations of active radicals are lower, and most of the fuel nitrogen is present in the form of NH_3 and HCN.
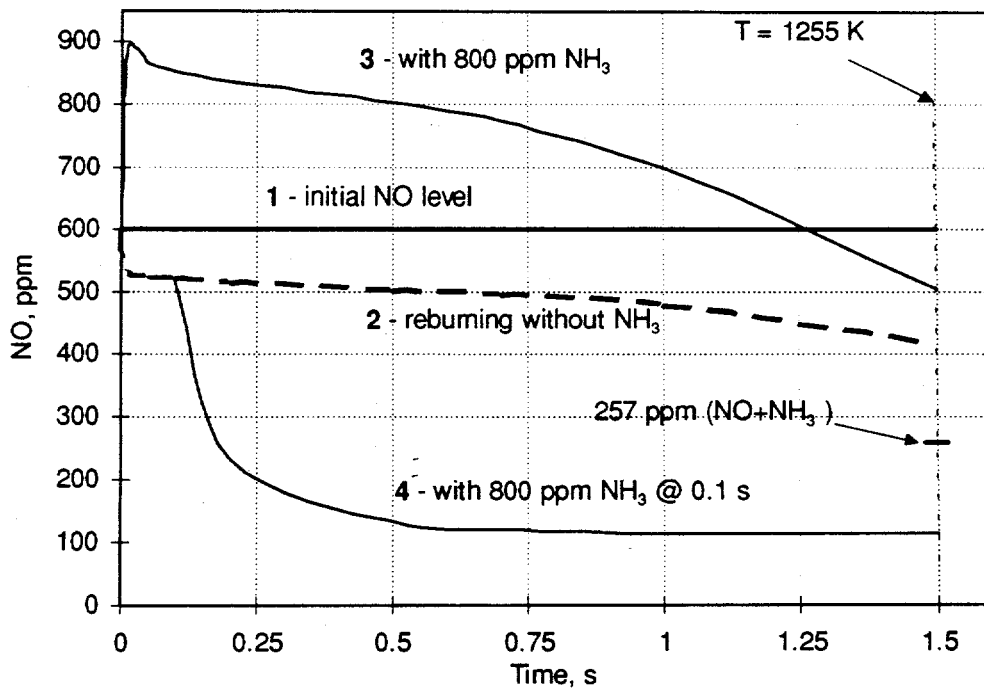
21

Figure 2.2.4. Effect of ammonia in the reburning zone at $SR_2 = 0.99$: 1 - initial NO level, 2 - reburning without ammonia, 3 - 800 ppm NH_3 co-injected with the reburning fuel, 4 - 800 ppm ammonia is added with 0.1 s delay time. TFN concentration (NO + NH_3 = 257 ppm) is shown at 1.5 s (the time of OFA injection at 1255 K).

2.3 Promotion of the NO-NH$_3$ Interaction in the Reburning Zone

Consideration of the kinetic curves of the reburning process (Figures 2.1.1 - 2.1.3) demonstrates that after the initial fast reaction stage, concentrations of main components in the reburning zone (CO, H$_2$ and NO at SR$_2$ = 0.99-0.95 and CO, H$_2$, CH$_4$, HCN, NH$_3$, NO at SR$_2$ = 0.90) remain almost constant, and, simultaneously, concentrations of radicals (OH and H) and O$_2$ decrease. The goal of modeling is to find conditions under which NO and TFN concentrations will decrease in the reburning zone. As was shown above, delayed injection of ammonia can reduce NO and TFN concentrations under certain conditions. The effectiveness of the NO-NH$_3$ interaction in the reburning zone can be further improved in the presence of promoters. The influence of different promoters (radicals, oxygen and fuels) on NO/TFN removal is analyzed in this Section. The second slow process in the reburning zone is considered, and parameters affecting the NO/TFN level are varied to find optimum conditions of NO/TFN removal. These parameters include the stoichiometric ratio in the reburning zone (SR$_2$); RF injection temperature (T$_i$); concentrations of ammonia, oxygen, radicals, and other compounds capable of promoting the NO-NH$_3$ interaction. It is clear that the influence of ammonia is different at various values of SR$_2$. Variation of process parameters was performed for SR$_2$ = 0.99 and 0.90 at a constant temperature gradient of 300 K/s. For all conditions, concentrations are shown at a reaction time of 1 s.

Initial modeling results on promotion of NO-NH$_3$ interaction in the reburning zone were obtained for injection of RF to provide SR$_2$ = 0.99. After the first fast reaction stage, all CH$_4$ was consumed, and concentrations of CO, H$_2$ and NO stabilized on a certain level. These conditions (mixture I)

500 ppm NO - 0.16% H$_2$ - 0.23% CO - 8% CO$_2$ - 15% H$_2$O - balance N$_2$

were considered as initial ones for the modeling study, and they correspond to the reaction time of about 0.1 s in Figure 2.1.1. At this initial point, ammonia and different promoters were added to mixture I.

Effect of ammonia addition to mixture I is shown in Figure 2.3.1. Without NH$_3$ injection (the upper
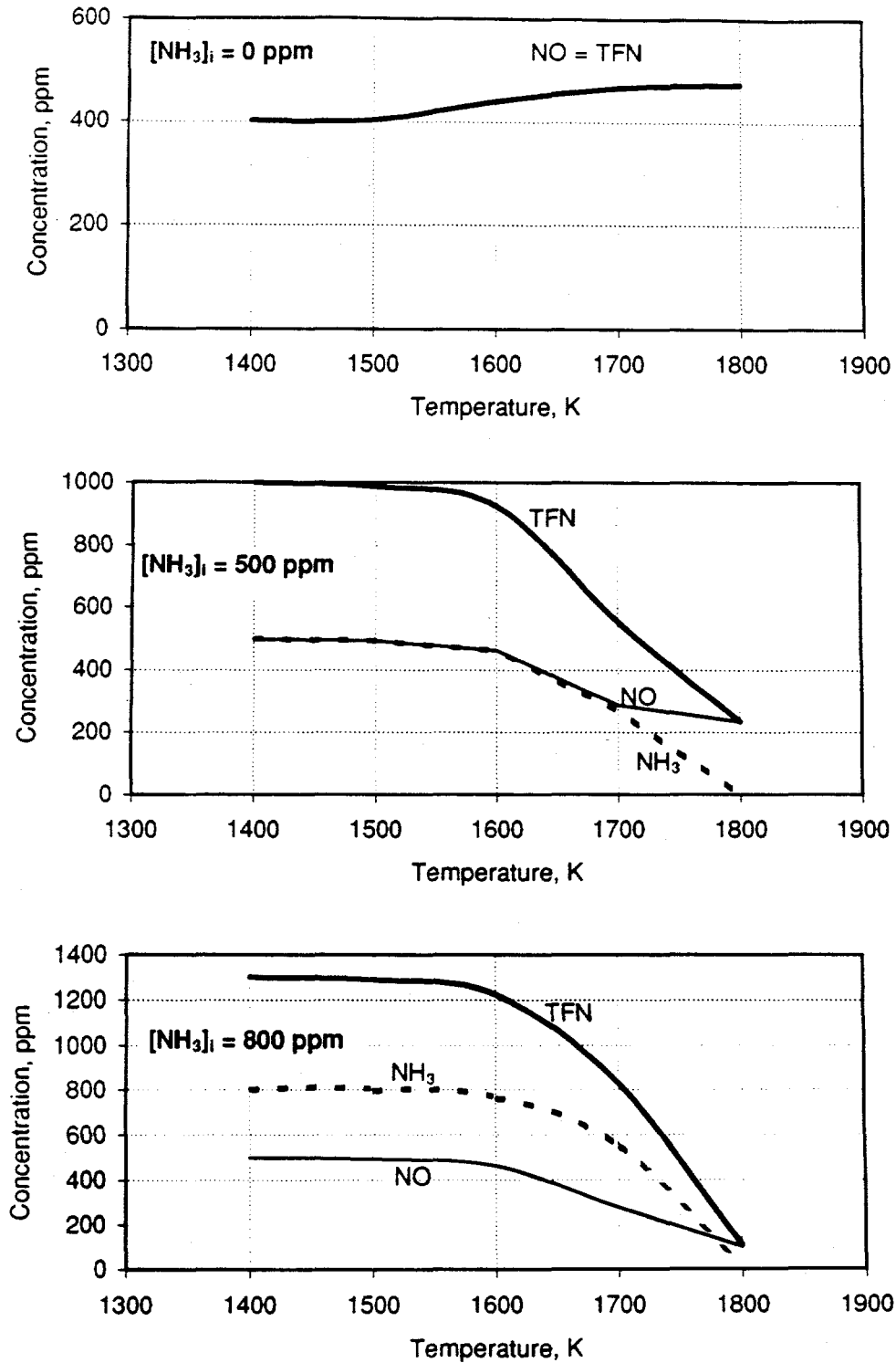
23

Figure 2.3.1. Effect of NH_3 injection temperature and NH_3 concentration in mixture I on NO/TFN reduction.

graph), NO is slightly reduced at lower NH_3 injection temperature. Injections of 500 and 800 ppm NH_3 (two other graphs) cause a TFN increase at lower temperatures and significant NO/TFN reduction at higher temperatures: 234 and 108 ppm TFN at 1800 K for 500 and 800 ppm NH_3 injection, respectively.

Performance of ammonia in the reburning zone greatly depends on the level of oxygen. If the oxygen concentration is high, NH_3 is partially converted to NO. If oxygen concentration is low, active radicals are not formed in oxidation processes. Thus, a maximum performance of NO/TFN removal should correspond to a certain optimum O_2 concentration. To determine this optimum O_2 concentration, calculations were performed with injection of 500 ppm NH_3 with various amounts of oxygen into mixture I. Figure 2.3.2 demonstrates the results. The optimum O_2 amounts depend on injection temperature and vary from 50 ppm at 1500 K to 120 ppm at 1700 K. Performance of TFN removal is greater at lower injection temperature: minimum TFN concentrations are 170 ppm at 1700 K and about 100 ppm at 1500 K.

Performance of other possible promoters was modeled by the same means: radicals (OH and H) and other compounds were co-injected with ammonia in different amounts into mixture I at 1600 K. Figure 2.3.3 compares effect of different additives: O_2, OH, H, O, O_2+OH, and O_2+H_2O_2. Though these promoters show different degrees of TFN removal, they perform not better than the injection of oxygen. Thus, oxygen participating in formation of different radicals via reactions with CO, H_2 and NH_3, shows better or about the same performance as other additives.

All promotive additives presented in Figure 2.3.3 were co-injected with ammonia, and thus, they appeared instantly in the gas phase. However, under real conditions, the promoters may be formed in the mixture with a certain rate constant. As has been proven by Zamansky and Borisov, 1992, the rate of promoter formation may be optimum, i.e. formation of promoters with a certain optimum rate constant results in maximum promotion effect. It was assumed for modeling that a hypothetic promoter X dissociates with formation of radicals or oxygen in the gas mixture. The following reaction was added to the mechanism:
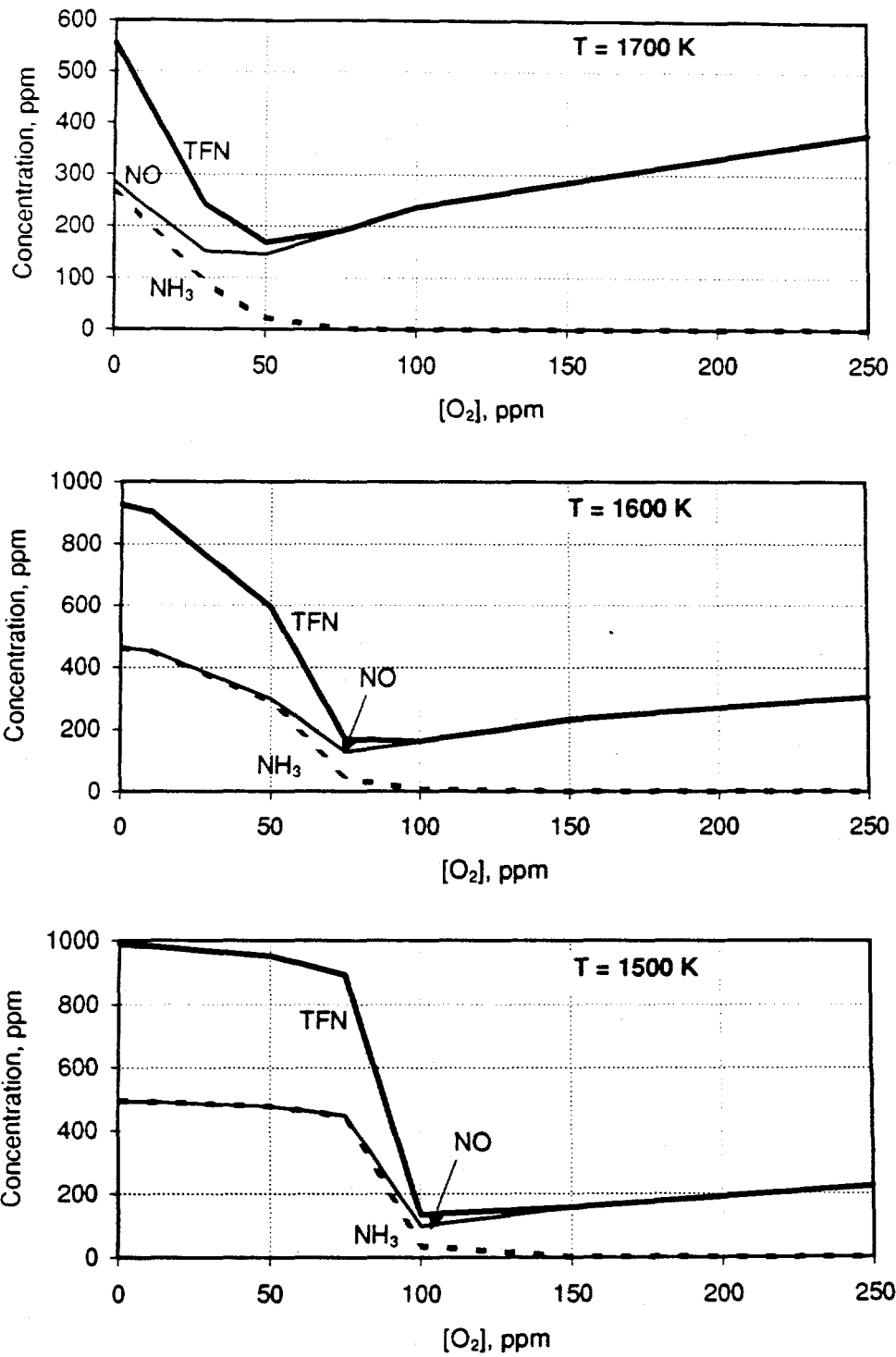
Figure 2.3.2. Effect of oxygen co-injection with 500 ppm NH_3 into mixture I at different injection temperatures.
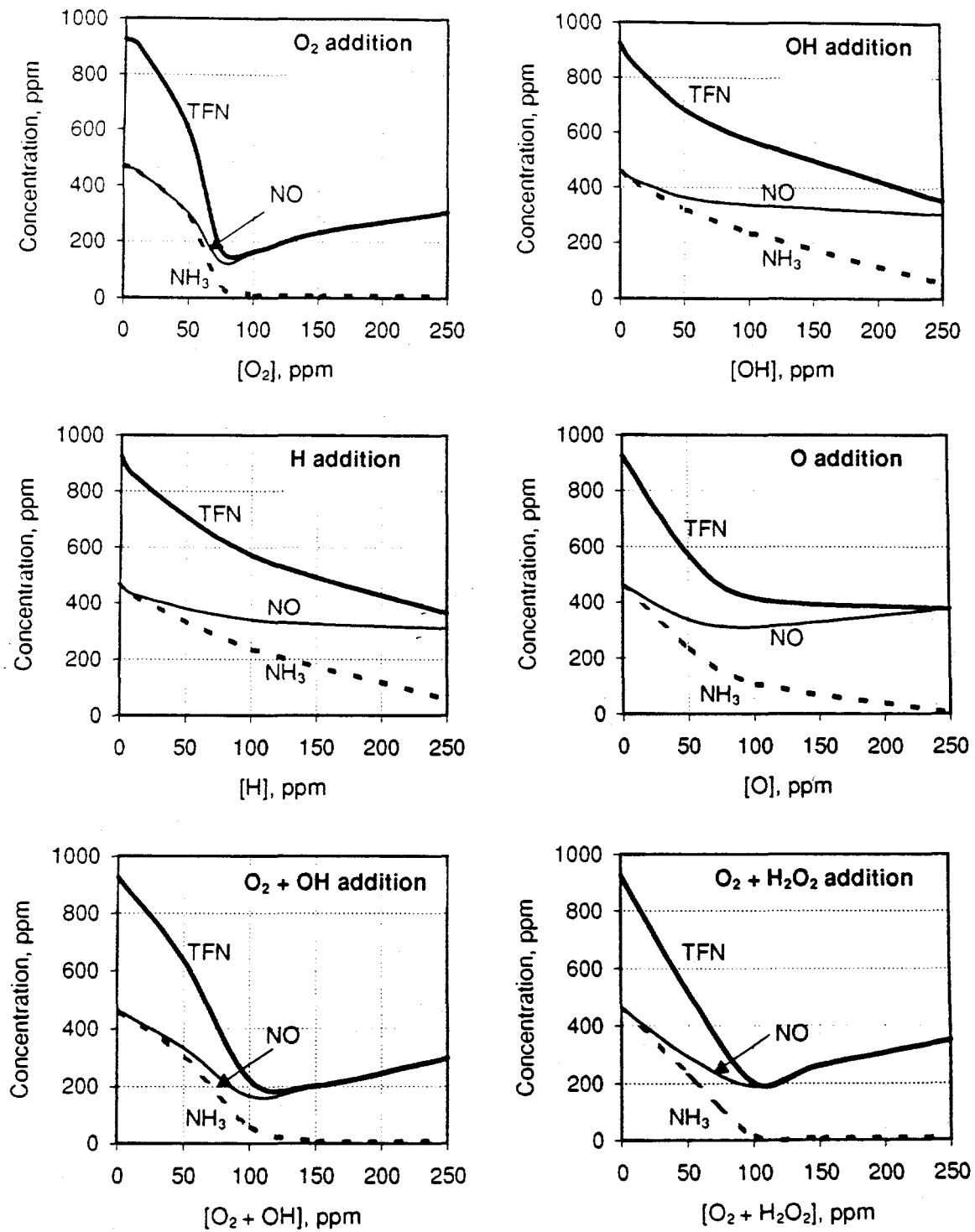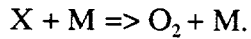
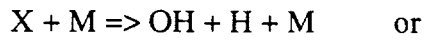Figure 2.3.3. Effect of radicals co-injection with 500 ppm NH₃ into mixture I, T₂ = 1600 K.

$$X + M => OH + H + M \qquad \text{or}$$

$$X + M => O_2 + M.$$

These equations simulate fast interaction of the hypothetic promoter X with water molecules or other species in flue gas with formation of OH, H, and O_2. The initial concentration of X was assumed to be 50 ppm in modeling. The rate constant for X decomposition was selected in the Arrenius form

$$k = A \cdot \exp(-20,000/T) \ cm^3/mol \cdot s$$

where the predexponential factor A was varied in the range from 10^9 to 10^{13}. These values of the rate constant provided formation of radicals and O_2 with characteristic times between approximately 0.1 and 100 s.

Figure 2.3.4 compares the results of modeling NO, NH_3 and TFN concentrations at different values of the factor A (i.e. depending on the rate of active species formation in the mixture) for three different cases: formation of OH+H radicals, formation of O_2, and formation of the OH/H radicals with co-injection of NH_3 and 75 ppm O_2. In a wide range of the promoter decomposition rate, NO and TFN concentrations are substantially lower than their values without promoter. In all cases, an optimum rate constant exists which results in minimum TFN concentration. The optimum factor A is in the range logA = 10.5-12.0. Oxygen formation and co-injection present the most attractive cases because the TFN minimum is lower.

Carbon-containing compounds can also provide radicals which promote the NO-NH_3 interaction in the reburning zone. Effect of different potential promoters on concentrations of NO, NH_3 and TFN is shown in Figure 2.3.5. This graph compares the effect of 500 ppm NH_3 injection into mixture I at 1600 K with co-injection of 100 ppm promoter: oxygen, methanol, methane, ethylene or ethane. One can see that the presence of oxygen provides best performance in comparison with other conditions examined.
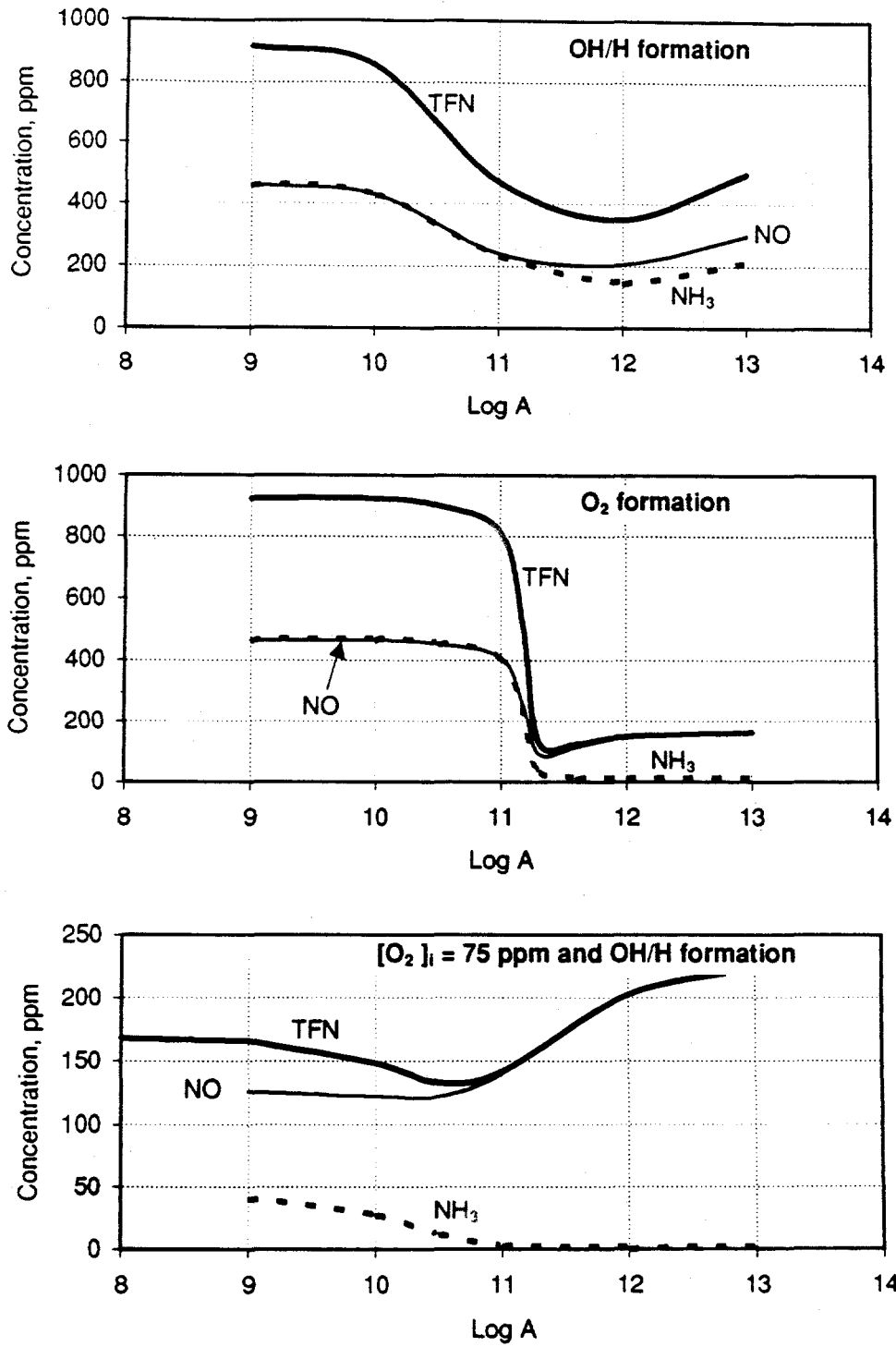
Figure 2.3.4. Modeling of the promotion effect at different predexponential factors A. The promoter appears with different rate constants in mixture I + 500 ppm NH_3 at T_1 = 1600 K.
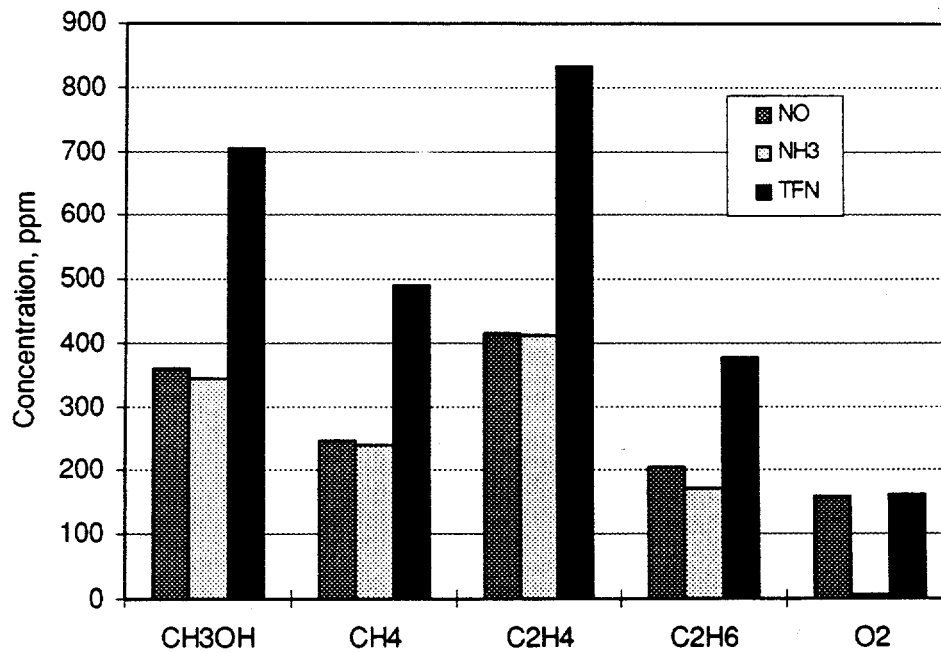
Figure 2.3.5. Comparison of the promotion effect of different compounds. The promoter (100 ppm) is co-injected with 500 ppm NH_3 into mixture I at $T_1 = 1600$ K and $SR_2 = 0.99$.

The modeling study makes it possible to select optimal conditions for reburning at $SR_2 = 0.99$. The calculated NO concentration profile under optimum conditions is shown in Figure 2.3.6, Curve 4. Figure 2.3.6 compares performance of the reburning process at $SR_2 = 0.99$ in the presence of NH_3, similar to Figure 2.2.4, but it represents conditions with highest performance achieved in modeling. The initial fast TFN reduction process is more efficient at lower temperature (Figure 2.1.7). Therefore, one can select a temperature of 1500 K for RF injection. This provides about 30% NO/TFN reduction, Curve 1. The NO concentration decreases to 400 ppm in 0.5 s. Curve 2 represents co-injection of 600 ppm NH_3 with the reburning fuel. The NO concentration drops, then slightly increases and finally slowly decreases to 480 ppm in 0.5 s. Curve 3 models injection of 500 ppm NH_3 after a 0.1 s delay time. In 0.5 s of the reaction time, the NO concentration drops to about 350 ppm.

Finally, if 500 ppm NH_3 and 100 ppm O_2 are injected with the 0.1 s delay time (Curve 4), the NO concentration decreases to 113 ppm and only 29 ppm NH_3 is left in the reaction media. Injection of OFA at 1320 K results in 138 ppm NO in the mixture as shown in Figure 2.3.6. These optimum condition cause 68% NO reduction by delayed injection of ammonia with the oxygen promoter into the reburning zone.

Kinetic curves of components in the reburning zone at $SR_2 = 0.90$ and $T_1 = 1700$ K are shown in Figures 2.1.3 and 2.1.5. The principal difference with the $SR_2 = 0.99$ case is that the reburning process is more efficient and there are three fuel-N products in the reburning zone: NO, HCN, and NH_3. For instance, at $t = 0.5$ s (Figure 2.1.3) their concentrations are the following: NO = 67 ppm, HCN = 76 ppm, $NH_3 = 116$ ppm, and TFN = 259 ppm. Concentration of the internally formed NH_3 is higher in modeling than that of NO and therefore, NH_3 injection is not necessary for further NO removal. One can notice (Figure 2.1.3) that O_2 disappears within first 0.02 s and concentrations of H and OH are lower than at $SR_2 = 0.99$ and 0.95 (Figures 2.1.1 and 2.1.2, respectively). Therefore, the reaction between the available NH_3 and NO does not proceed, and their concentrations are almost constant within reaction times from 0.1 to 0.5 s. To activate the internal NH_3, active species should be regenerated in the reburning zone and injection of oxygen can help to do it.

31
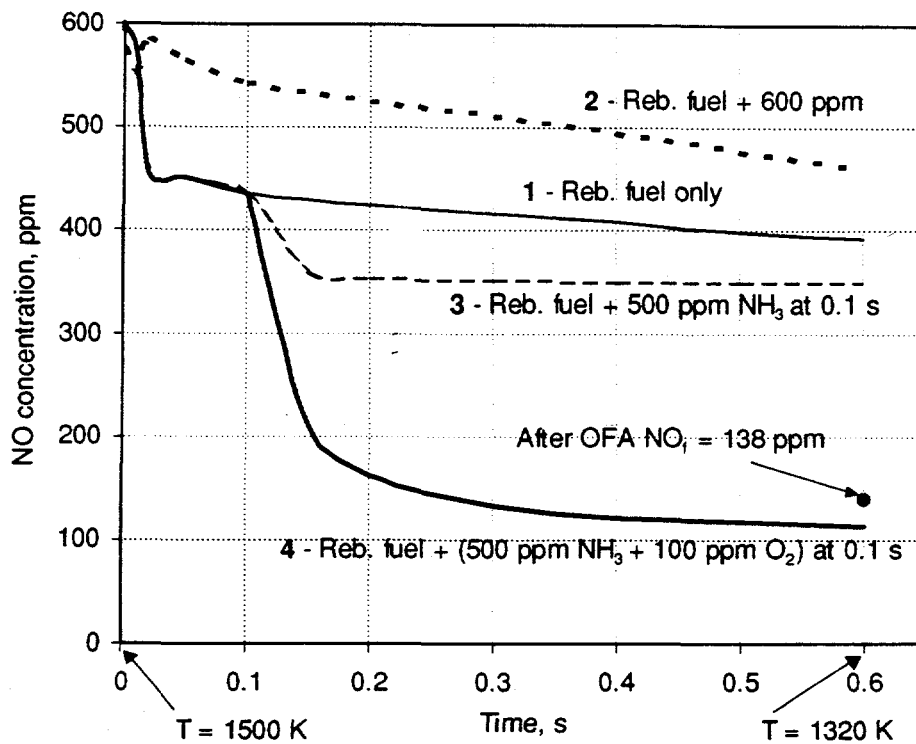
Figure 2.3.6. Optimum conditions for NO removal at $SR_2 = 0.99$: 1 - injection of reburning fuel only at 1500 K, 2 - co-injection of 500 ppm ammonia with the reburning fuel, 3 - injection of 500 ppm NH_3 with a 0.1 s delay time, 4 - delayed injection of 500 ppm ammonia with 100 ppm O_2. Final NO concentration (NO_f = 138 ppm) is shown at the time of OFA injection at 1320 K.

Figure 2.1.7 shows that at $SR_2 = 0.90$ the efficiency of reburning is higher at higher RF injection temperature. Therefore, modeling was conducted at $T_1 = 1700$ K. Different amounts of oxygen were injected in the reburning zone with various delay times. Figure 2.3.7 demonstrates the resulting concentrations of CO, H_2 and fuel-N species for injection of oxygen into the reburning zone at 1600 K that corresponds to a 0.33 s delay time. Concentrations are shown at $t = 1.0$ s, i.e. $T = 1300$ K. TFN concentration has a wide minimum in the range of oxygen level between 0.1 and 0.6%. TFN can be reduced to about 85 ppm if 0.3-0.4% O_2 is injected into the reburning zone. This concentration corresponds to a fuel rich mixture with CO/H_2 concentrations within 1.5 - 1.8% range. Injection of higher O_2 concentrations causes less efficient TFN removal and at $[O_2] = 2\%$, all CO and H_2 species are consumed and some oxygen, about 150 ppm, is present in the mixture at the reaction time of 1 s.
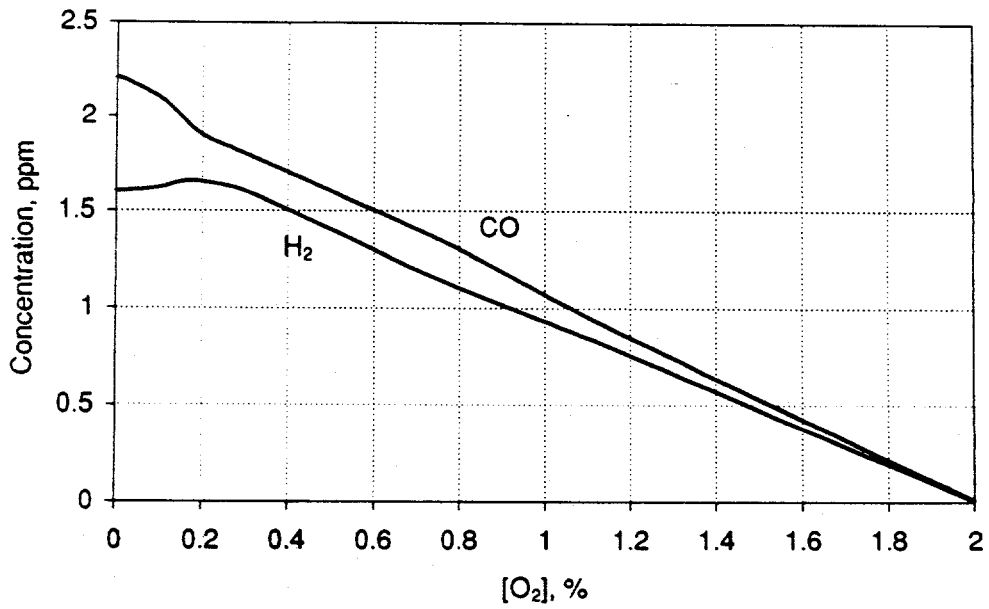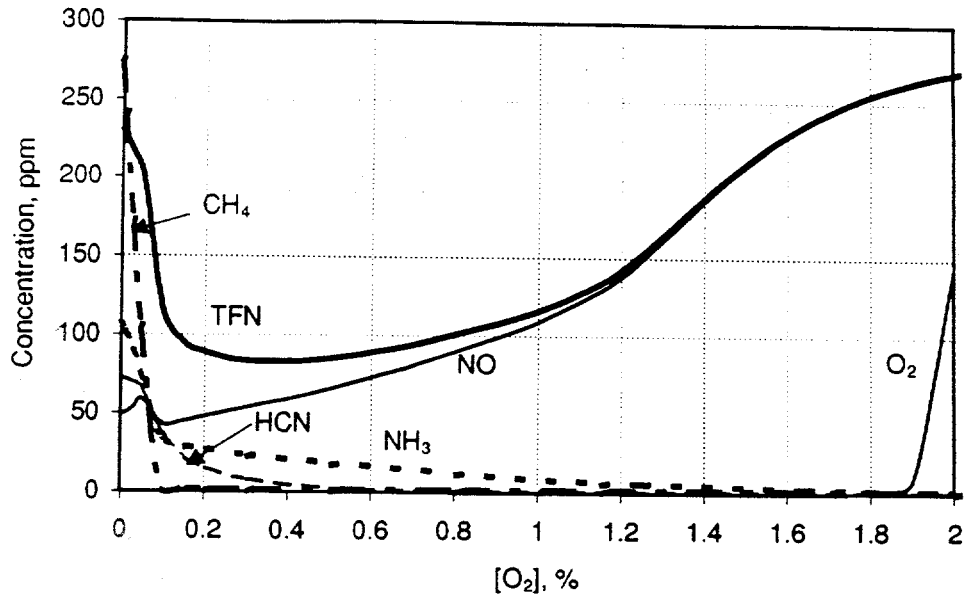
Figure 2.3.7. Efficiency of reburning at $SR_2 = 0.90$ and $T_1 = 1700$ K depending on different O_2 amounts injected with a 0.33 s delay time (at 1600 K) into the reburning zone.

3.0 Kinetics of Sodium Reactions

(Summary of activities at the University of Texas, March 1996)

As a subcontractor to EER, The University of Texas at Austin is responsible for the experimental study and theoretical modeling of processes of decomposition of salts of alkali metals, as proposed as prospective additives for NO_x removal from flue gases. The University of Texas at Austin will also study interactions of these salts with components of flue gases (CH_4, CO, NO, NH_3, H_2, H_2O, O_2, and SO_x). Significant experimental and modeling efforts are required for successful fulfillment of the project, and first step in coordination of theses efforts is development of a two year plan of the work. We developed the following plan for the work to be conducted at the University of Texas.

Task 1.2 Kinetics of Na_2CO_3 Reaction with Flue Gas Components, 3/96 - 9/97

General Objective: To confirm and develop the technical basis of the promotor additive Na2CO3. Quarterly Reports for periods ending: March 31, June 30, September 30, December 31

3/96 - 6/96

Literature review on Na_2CO_3 reactions at high temperatures.
Reconstruction of flow system and construction of gas handling system for gas chromatograph (GC).
Quarterly Report.

7/96 - 12/96

Development of a Na_2CO_3 solution injection system, calibration of the injection system. Flow system study of Na_2CO_3 decomposition. Reactions of Na_2CO_3 with components of flue gas. Method: GC detection of CO_2 and other components of flue gas.
Quarterly Reports.

1/97 - 3/97

Kinetic modeling of Na_2CO_3 decomposition in the presence of flue gas components.

Experimental study of reactions of other sodium salts ($NaHCO_3$, CH_3COONa) with flue gas components.

Quarterly Report.

4/97 - 6/97

Development of a kinetic model of the reaction between Na_2CO_3 and flue gas components. Shock tube study of Na_2CO_3 reactions with flue gas components. Method: GC analysis of products and optical detection of Na atoms.

Quarterly Report.

Final Report.

A detailed literature review on the high temperature reactions of Na_2CO_3 was started in March; the results will be reported in the next Quarterly Report. Experimental efforts were started with the construction of the flow and gas handling systems for GC analysis. The gas handling system was constructed from glass and metal components to enable high and low pressure operation. Existing GC columns were replaced with new columns packed with molecular sieves and HAYESEP Q to enable measurements of CO_2 (presumed to be the main product of Na_2CO_3 decomposition) and surrogate components of flue gas.

The GC gas handling system is in operating conditions and calibrations have begun; reconstruction of the flow system to facilitate Na_2CO_3 injection has not started yet. Preliminary runs showed that the detection limit of the flame ionization detector is 50 ppm when CH_4 is taken as reference gas and that the sensitivity of the thermal conductivity detector is 600 ppm when O_2 is taken as reference gas.

In the next three months experimental efforts will be directed on reconstruction of the flow system.

4. 0 Conclusions

The modeling study on chemical behavior of ammonia in the reburning zone makes it possible to conclude that:

1. Injection of the reburning fuel at SR_2 of about 0.90 and lower generates NH_3 and HCN, but at $SR_2 = 0.99$-0.92, NO are the principal fuel-N species in the reburning zone. Reburning is more efficient at lower RF injection temperature within a range of SR_2 between 0.99-0.95. At higher RF concentrations, NH_3 and HCN become a substantial part of fuel-N species, and the efficiency of the process becomes higher at higher RF injection temperatures.

2. There are two steps of NO reduction in the reburning zone. The first fast step, about 5 ms at 1700 K, involves reactions of C-containing radicals. Among them, HCCO and CH_2 are the most important srecies. During the second step, NO slowly reacts with N-species.

3. Delayed NH_3 injection into the reburning zone is efficient at $SR_2 = 0.95$-0.99 and the most efficient at near stoichiometric conditions, $SR_2 = 0.99$. Short delay times, about 0.1 s, and NSR_1 of about 1.2-1.3 are preferable at $SR_2 = 0.99$ and provide higher NO/TFN control efficiency.

4. At $SR_2 = 0.99$, promoters, co-injected with ammonia, are capable of reducing NO concentration. Small oxygen concentrations can activate the NO/NH_3 interaction, and they are the most efficient among promotive additives examined. The promotion effect is higher at lower injection temperatures and at the level of O_2 injected of 50-150 ppm. Formation of O_2 and other promoters in the reburning zone from different additives with certain rate constants can increase NO control efficiency. Under optimum conditions at $SR_2 = 0.99$, NO can be reduced by about 80% via promoted injection of ammonia into the reburning zone.

5. At $SR_2 = 0.90$, ammonia is formed in the reburning zone and can react with NO if the system is activated by injection of 0.1-0.4% O_2. The oxygen injection is more efficient at small delay times of about 0.1 s. At $SR_2 = 0.90$, TFN concentration can by reduced via oxygen (air) injection into the reburning zone by about 88%.

5.0 Future Plans

The main activities of the next quarter will include continuation of the parametric experiments with the use of the bench-scale 0.1 MBtu/hr combustion facility. Modeling will be focused on ammonia injection into the burnout zone and on sensitivity analysis to define most important elementary reactions under different conditions. Experimental program at the University of Texas will also be continued. Results will be presented at the First Joint Power and Fuel Systems Contractors Conference July 9-11, 1996 in Pittsburgh and at the 1996 AFRC (American Flame Research Committee) International Symposium, Baltimore, MD, September 30 - October 2, 1996.

6.0 References

Bowman, C.T., SNCR Mechanism, private communication, October, 1995.

Bowman, C.T., Hanson, R.K., Davidson, D.F., Gardiner, W.C.Jr., Lissianski, V.V., Smith, G.P., Golden, D.M., Frenklach, M., Wang, H. and Goldenberg, M., http://www.gri.org, 1995.

Kee, R.J., Rupley, F.M. and Miller, J.A., Chemkin-II: a Fortran Chemical Kinetics Package for the Analysis of Gas-Phase Chemical Kinetics, Sandia National Laboratories Report No. SAND89-8009, 1989.

Zamansky, V.M. and Borisov, A.A., Promotion of High-Temperature Self-Ignition, Prog. Energy Combust. Sci., V. 18, pp. 297-325, 1992.

Zamansky, V.M. and Maly, P.M., Second Generation Advanced Reburning for High Efficiency NOx Control, EER 1st Quarterly Report, DOE Contract No. DE-AC22-95PC95251, January, 1996.